

Fouling behaviours of two stages microalgae/membrane filtration system applied to palm oil mill effluent treatment

Yeit Haan Teow^{*1,2}, Zhong Huo Wong^{2a}, Mohd Sobri Takriff^{1,2b} and Abdul Wahab Mohammad^{1,2b}

¹Research Centre for Sustainable Process Technology (CESPRO), Faculty of Engineering and Built Environment, Universiti Kebangsaan Malaysia, 43600 Bangi, Selangor, Malaysia

²Chemical Engineering Programme, Faculty of Engineering and Built Environment, Universiti Kebangsaan Malaysia, 43600 Bangi, Selangor, Malaysia

(Received March 22, 2016, Revised January 22, 2018, Accepted January 24, 2018)

Abstract. Fouling by solids and microorganisms is the major obstacle limiting the efficient use of membrane wastewater treatment. In our previous study, two stages microalgae/membrane filtration system was proposed to treat anaerobic digested palm oil mill effluent (AnPOME). This two stages microalgae/membrane filtration system had showed great potential for the treatment of AnPOME with high removal of COD, NH₃-N, PO₄³⁻, TSS, turbidity, and colour. However, fouling behavior of the membrane in this two stages microalgae/membrane filtration system was still unknown. In this study, empirical models that describe permeate flux decline for dead-end filtration (pore blocking - complete, intermediate, and standard; and cake layer formation) presented by Hermia were used to fit the experimental results in identifying the fouling mechanism under different experimental conditions. Both centrifuged and non-centrifuged samples were taken from the medium with 3 days RT intervals, from day 0 to day 12 to study their influence on fouling mechanisms described by Hermia for ultrafiltration (UF), nanofiltration (NF), and reverse osmosis (RO) filtration mode. Besides, a more detailed study on the use of resistance-in-series model for dead-end filtration was done to investigate the fouling mechanisms involved in membrane filtration of AnPOME collected after microalgae treatment. The results showed that fouling of UF and NF membrane was mainly caused by cake layer formation and it was also supported by the analysis for resistance-in-series model. Whereas, fouling of RO membrane was dominated by concentration polarization.

Keywords: membrane process; fouling; Hermia's model; resistance-in-series; microalgae treatment

1. Introduction

Palm oil mill effluent (POME) is the single largest source of industrial wastewater pollution in Malaysia (Li *et al.* 2011), which being the second largest oil palm producing country after Indonesia. POME poses a great threat to the water quality of the environment nearby due to oxygen depletion and enormous pollution problem. So with the increasingly stringent current and future water quality regulations, progress has been made in improving the current POME treatment process.

In our previous study, a new approach of two stages microalgae/membrane filtration system designed with integrates microalgae pretreatment and membrane filtration has been put forward and evaluated in promoting the recycling of treated anaerobic digested palm oil mill effluent (AnPOME) for internal plant usage. During microalgae treatment, the microalgae can restore the oxygen in AnPOME, as a means of substituting freshwater while concomitantly ingest ammonia nitrogen (NH₃-N) and orthophosphorus (PO₄³⁻) as essential nutrients for the

metabolism and growth of microalgae during photosynthesis. Whereas for membrane, it was further employed as an innovative technology for the purpose of water recycling but a decline in membrane performance over a period of time due to membrane fouling is still a critical problem. In this way, quantification of the effect of basic parameters (microalgae retention time (RT), membrane filtration mode) on membrane fouling should be accomplished to quantitatively describe membrane filtration process dynamics for the economic and technological point view of this two stages microalgae/membrane filtration process.

Membrane fouling can involve several distinct phenomena. These phenomena can be desirable or undesirable, reversible or irreversible, which are characterized by mechanism and location. If the membrane pores are larger than the size of the solute molecules, these molecules can enter the membrane pores causing internal pore fouling. Thus, pore size is reduced and pore flow is constricted. Internal pore fouling is usually difficult to clean. When the opposite occurs, the membrane pores are smaller than the size of the solute molecules present in the feed solution, these molecules will accumulate over the membrane surface causing pore sealing and/or the formation of a gel layer. Whereas, solute molecules of similar size to that of the membrane pores may result in a partial blocking.

*Corresponding author, Ph.D.

E-mail: yh_teow@ukm.edu.my

^aM.Sc. Student

^bProfessor

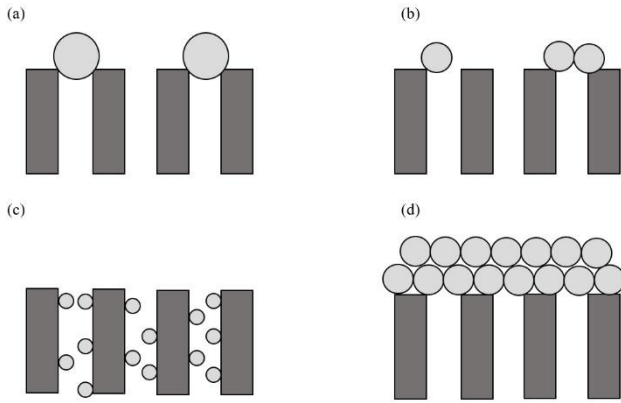


Fig. 1 Schematic drawing of the porous membrane fouling mechanism (a) complete blocking (b) intermediate blocking (c) standard blocking and (d) cake layer formation

In this work, the empirical models that describe permeate flux decline for dead-end filtration (pore blocking—complete, intermediate, and standard; and cake layer formation) presented by Hermia (Hermia 1982) were used to fit the experimental results in identifying the fouling mechanism under different experimental conditions. Both centrifuged and non-centrifuged samples were taken from the medium with 3 days RT intervals, from day 0 to day 12 to study their influence on fouling mechanisms described by Hermia for ultrafiltration (UF), nanofiltration (NF), and reverse osmosis (RO) filtration mode. Besides, this paper also provides a more detailed study on the use of resistance-in-series model for dead-end filtration to investigate the fouling mechanisms involved in membrane filtration of AnPOME collected after microalgae treatment. While most of the literature reports on one filtration mode, in this paper the experimental conditions were varied to a large extent so that the effect of different membrane filtration mode on fouling mechanism can be compared. Thus, different fouling mechanisms that might occur at different filtration process may be found.

2. Theoretical background

Hermia (1982) developed four empirical models for dead-end filtration based on constant pressure filtration laws that corresponded to four basic types of fouling: complete blocking, intermediate blocking, standard blocking, and cake layer formation. The parameters considered by these models have a physical meaning and contribute to the comprehension of the mechanisms of membrane fouling.

$$\frac{d^2t}{dV^2} = K \left(\frac{dt}{dV} \right)^n \quad (1)$$

where V is the cumulative permeate volume (m^3), t is the filtration time (s), and K is a proportionality constant. Typical values for the parameter n depending on the type of fouling: complete blocking ($n = 2$), intermediate blocking ($n = 1$), standard blocking ($n = 1.5$), and cake layer formation ($n = 0$). Fig. 1 illustrates the different fouling mechanisms.

2.1 Complete blocking model ($n = 2$)

Complete blocking model assumes that every molecule that reaches the membrane surface completely blocks the entrance of the membrane pores such that the molecules are never superimposed upon the other. This creates a single layer of particles blocking all pores on the membrane surface but not within the pores. Considering these two hypotheses, Hermia (1982) concluded that n was equal to 2 in this case.

For $n = 2$, Eq. (1) linearized and expressed in terms of the permeate flux versus time results in Eq. (2) (Lim and Bai 2003).

$$\ln J_p = \ln J_o - K_c t \quad (2)$$

where J_p is the permeate flux (m/s), J_o is the initial permeate flux (m/s), and K_c is the constant corresponded to the complete blocking model (/m). The parameter K_c can be expressed as a function of the membrane surface blocked per unit of the total volume that permeates through the membrane, K_A , and as a function of J_o , according to Eq. (3) (Bowen *et al.* 1995). Therefore, the active membrane surface decreases as a consequence of their pores being completely blocked (de Barros *et al.* 2003).

$$K_c = K_A J_o \quad (3)$$

2.2 Standard blocking model ($n = 1.5$)

In standard blocking model, the molecules diameter is much smaller than the pore diameter, thus, the molecules can enter most pores, deposited over the pore walls. As a result, the volume of membrane pores decreases proportionally to the filtered permeate volume.

For the standard blocking model, permeate flux as a function of time is given by the linearized Eq. (4) (Bowen *et al.* 1995).

$$\frac{1}{\sqrt{J_p}} = \frac{1}{\sqrt{J_o}} + K_s t \quad (4)$$

where K_s is the constant corresponded to the standard blocking model ($1/\sqrt{\text{m}\cdot\text{s}}$). The parameter, K_s , is defined in Eq. (5), which depends upon the volume of molecules retained per unit permeate unit.

$$K_s = 2 \frac{K_B}{A_o} A \sqrt{J_o} \quad (5)$$

where K_B is the parameter in the standard blocking model that represents the decrease in the cross-sectional area of membrane pores per unit of the total volume permeated through the membrane (/m), A is the membrane area (m^2), and A_o is the membrane porous surface (m^2).

2.3 Intermediate blocking model ($n = 1$)

Almost similar to the complete blocking model, this model considers that, when a molecule approaches an open membrane pore, the molecule blocks the pore. However, intermediate blocking model is less restrictive in such a way that not every molecule that arrives to the membrane

surface blocks a membrane pore. It considers that some molecules may deposited on other molecules that previously settled. This model examines the probability of a molecule to block a membrane pore. Considering these hypotheses, Hermia (1982) concluded that n was equal to 1 in this case.

Mohammadi *et al.* (2003) linearized Eq. (1) for n equal to 1 and expressed it in terms of permeate flux as a function of time.

$$\frac{1}{J_p} = \frac{1}{J_o} + K_i t \quad (6)$$

where K_i is the constant that corresponded to the intermediate blocking model (/m). The parameter K_i can be expressed as a function of blocked membrane surface per unit of the total volume that permeates through the membrane, K_A (Eq. (7)) (Bowen *et al.* 1995). The membrane surface that is not blocked is diminishes with time (Koltuniewicz and Field 1996). Consequently, the probability of a molecule blocking a membrane pore continuously decreases with time.

$$K_i = K_A \quad (7)$$

2.4 Cake layer formation model ($n = 0$)

The cake layer filtration model is used to explain for the case of large solute molecules which built up multiple layers, causing resistance to the flow of fluid through the membrane. The linearized equation for permeate flux with time is the following (Lim and Bai 2003):

$$\frac{1}{J_p^2} = \frac{1}{J_o^2} + K_{gl} t \quad (8)$$

where K_{gl} is the constant corresponded to the cake layer formation model (s/m^2). The parameter K_{gl} is given by Eq. (9) (Bowen *et al.* 1995), which depends on both cake resistance and concentration.

$$K_{gl} = \frac{2R_g K_D}{J_o R_m} \quad (9)$$

where R_m is the membrane resistance (/m).

2.5 Resistance-in-series model

While Hermia's model is good in identifying the predominant mechanism during fouling, resistance-in-series model which also apply Darcy's law able to find out the dominant resistance components that caused the flux decline. Resistance-in-series model has four factors in explaining the membrane fouling: membrane hydraulic resistance (R_m), concentration polarization resistance (R_c), cake layer resistance (R_g), and adsorption resistance (R_a).

$$J = \frac{\Delta P}{\mu(R_m + R_g + R_c + R_a)} = \frac{\Delta P}{\mu R_t} \quad (10)$$

The three resistances in the equation are operationally defined and can be identified as follow: R_m was measured by filtering pure water through new membrane at constant pressure assuming R_g , R_c , and R_a were zero. With the known

ΔP and μ , R_m can be calculated using Eq. (11).

$$J_{membrane} = \frac{\Delta P}{\mu R_m} \quad (11)$$

R_i was measured from the operational data that was obtained from actual feed solution filtration.

$$J_{total} = \frac{\Delta P}{\mu R_t} \quad (12)$$

After that, the actual feed solution was removed and pure water was added back for filtration again. In this case, $R_m + R_g + R_a$ was calculated by eliminating the R_c from $R_m + R_g + R_c + R_a$. Due to no solute molecules in pure water during filtration, no concentration gradient occurred which leads to back-transport of the fluids.

$$J_{without R_c} = \frac{\Delta P}{\mu(R_m + R_g + R_a)} \quad (13)$$

After cleaning the membrane by peeling off the cake layer, filtration can be performed to obtained $R_m + R_a$. It is assumed that after the cake layer was removed, only the irreversible R_a and R_m are actually causing the fouling.

$$J_{without R_g} = \frac{\Delta P}{\mu(R_m + R_a)} \quad (14)$$

3. Experimental methods

3.1 Materials

Three different types of flat sheet commercial membranes were purchased from Amfor Inc., Beijing, China. As reported by the manufacturer, ultrafiltration (UF) membrane, PES10 was made by polyethersulphone (PES) with the nominal molecular weight cut-off (WMCO) of 10 kDa and pH resistance ranging from 1 to 13. While for hydrophilic nanofiltration (NF) membrane, NF2 and reverse osmosis (RO) membrane, LE were made by polyamide (PA) thin film composite with 95% $MgSO_4$ and 99.4% NaCl rejection, respectively.

The feed solution used for membrane filtration was AnPOME collected after microalgae treatment in our previous study. Both centrifuged and non-centrifuged samples were taken from the medium with 3 days RT intervals, from day 0 to day 12 with the centrifugation speed of 8000 rpm for 5 minutes. The typical characteristics of these samples are summarized in Table 1.

3.2 Membrane filtration system

A laboratory bench-scale dead end test unit was used to study the performance of each membrane (UF, NF, RO) on both centrifuged and non-centrifuged effluent under different RT from microalgae treatment. The set-up of the dead-end membrane filtration test unit is depicted in Fig. 2. The unit mainly consisted of a membrane dead-end filtration cell, HP4750 (Sterlitech Corporation, WA, USA) with processing volume up to 300 mL, nitrogen gas to exert pressure on the permeation cell was controlled and monitored by a pressure gauge meter, stirrer to form a

Table 1 Typical characteristics of AnPOME after microalgae treatment at different retention time

Retention Time (Day)	Centrifugation	pH	COD (mg/L)	NH ₃ -N (mg/L)	PO ₄ ³⁻ (mg/L)	TSS (mg/L)	Turbidity (NTU)
Day 0	Yes	7.78	2764.00	265.25	378.13	243.3	112.0
	No	7.80	3390.00	294.00	580.00	1186.0	366.0
Day 3	Yes	8.44	1936.27	190.00	300.00	198.3	34.1
	No	8.49	2238.30	215.30	390.00	401.7	98.1
Day 6	Yes	8.88	1608.10	190.30	307.50	189.7	36.1
	No	8.92	1933.30	195.70	414.20	471.7	124.0
Day 9	Yes	9.04	1522.77	167.70	304.20	170.0	36.7
	No	9.08	1867.92	179.70	416.70	508.7	154.0
Day 12	Yes	9.18	1403.30	144.00	285.00	156.0	38.1
	No	9.22	1812.92	160.30	469.20	561.0	219.7

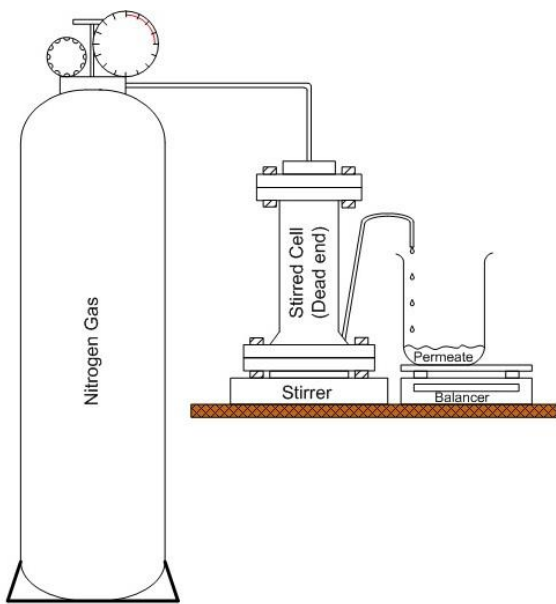


Fig. 2 Experimental set-up of dead-end membrane filtration

homogeneous feed inside the permeation cell throughout the membrane filtration process, and balance with data acquisition system for measuring filtrate flow.

All UF, NF, and RO flat sheet membranes were cut into the shape of disc with a diameter of 4.9 cm and the effective membrane filtration area was 14.6 cm² (excluding the area covered by the O-ring). The newly cut membrane was soaked in pure water and was left for a day to ensure complete removal from residual solvent/chemical. The membrane filtration test was performed by laying the front smooth surface of membrane facing the top of the membrane holder in the membrane test cell and then was tightened by a rubber O-ring. Different transmembrane pressures (TMP) was applied for each membrane, which is 5 bars, 7 bars, and 10 bars for UF, NF, and RO membrane, respectively. In order to alleviate the impact of compaction, pre-filtration study with pure water was first conducted at each respective TMP for 30 minutes until a steady-state flux was achieved. During the experiment, the AnPOME from

microalgae treatment was poured into the dead-end filtration cell unit. The permeate flux was measured for every 30 mL of permeate collected. The permeate flux, J was calculated by the following equation:

$$J = \frac{V}{A\Delta t} \quad (15)$$

where V (m³) is the volume of permeate water, A (m²) is the membrane area, and Δt (h) is the operating time.

4. Results and discussion

4.1 Effect of retention time (RT) and centrifugation on permeate flux profiles

Permeate flux profile of a membrane filtration process is the most common way to identify the occurrence of fouling phenomenon. The performance of the two stages microalgae/membrane filtration system was studied by altering the membrane filtration mode (UF, NF, RO) and the microalgae treatment RT. The permeate flux profiles resulting from successive filtration of AnPOME collected after microalgae treatment are illustrated in Fig. 3-5.

4.1.1 Ultrafiltration (UF)

By comparing the water permeation of UF membrane in filtering the centrifuged and non-centrifuged microalgae treated effluent, UF membrane gave a higher water flux of 10.64–12.35 L/m² h with centrifuged microalgae treated effluent filtration; whereas, a lower water flux of 7.97–11.25 L/m² h was achieved by UF membrane of non-centrifuged microalgae treated effluent filtration, showing that centrifugation of microalgae treated effluent before membrane filtration process had enhanced the permeation flux to certain degrees almost regardless to the microalgae treatment RT. It was proposed that the centrifugation of microalgae treated effluent helped greatly in reducing the total suspended solids (TSS) content in microalgae treated effluent as centrifugation will separate those solids and biomass which were heavier than the medium. Therefore, during membrane filtration process, fewer pores were blocked by suspended solids (SS) and other biomass aggregates that depositing on the membrane surface which obstructed the water molecules towards entrance of the available pores was lesser thus resulted in higher flux. This postulation was further supported by the research study of Turano and team (2002) in the treatment of olive mill wastewater. Turano and team (2002) used centrifugation as pretreatment in removing the SS prior an actual selective separation phase carried out by UF. The combination of centrifugation and UF resulted 13 times higher permeate fluxes compared to the feed solution without preliminary centrifugation.

Besides, Fig. 3a showed a slight rise in water flux as the RT of microalgae treatment was prolonged. The water flux was recorded as 11.23 L/m² h at day 0 of microalgae treatment RT and it was eventually increased to 12.35 L/m² h at day 12 of microalgae treatment RT. As the microalgae treatment RT was prolonged from day 0 to day 12, there was larger microalgae population inside the medium. The

growing of microalgae population will promote to the removal of SS as microalgae exudates which known as extracellular polymeric substances (EPS) that produced by microalgae with strong with adsorption properties that helps in anchoring the smaller particulates to the cell wall of the microalgae and removed together during centrifugation (Czaczyk and Myszka 2007). This finding was supported by the work of Hoskins and team (Hoskins *et al.* 2003), who claimed that a microorganism was able to produce polysaccharide-like polymers, such as carbohydrates and ammonium ions to help in trapping the nutrients, as an aid for surface attachment. These polysaccharide-like polymers contain organic matter, like neutral carbohydrates, uronic acids, and proteins, which will be removed together with microalgae during the centrifugation (Czaczyk and Myszka 2007).

However, by referring to Fig. 3b, permeate water flux profile of UF membrane in filtering the non-centrifuged microalgae treated effluent showed a diverse trend compared to permeate water flux profile of UF membrane in filtering the centrifuged microalgae treated effluent in Fig. 3a. Results in Fig. 3b showed that the initial prolong of microalgae treatment RT was apparently enhanced the permeate water flux with the highest water flux of 11.25 L/m² h was achieved at day 3 of RT. This is probably due to the high adsorptive properties of EPS molecules which bind those small particulates into the exudates of microalgae, thus prohibiting them from passage through the membrane and blocked the UF membrane's pores. Due to such incident, large hydrodynamic radius EPS molecules approach the membrane surface will provide some void and less restrictive in such a way that fewer free small particulate could enter the membrane pores and deposited over the pore walls. As a result, volume of filtered permeate was increased. When the microalgae treatment RT was increased from day 3 to day 12, massive amount of microalgae biomass would have higher cake layer formation. Built up of multiple cake layers will hindered the flow of water through UF membrane, resulting in lower permeate flux through the membrane.

4.1.2 Nanofiltration (UF)

From Fig. 4, the flux profile of NF membrane in filtering the centrifuged and non-centrifuged microalgae treated effluent, it can be notify that NF membrane results a contrary trend compared to UF membrane for microalgae treated effluent at day 0 of RT in which higher water flux of 7.62 L/m² h was recorded of non-centrifuged microalgae treated effluent filtration; whereas, lower water flux of 5.20 L/m² h was achieved by NF membrane of centrifuged microalgae treated effluent filtration, meaning that centrifugation of microalgae treated effluent at day 0 of RT before membrane filtration process had brought negative impact to the permeation flux. This phenomenon can be explained by the differences of UF and NF membrane pore size in filtering the microalgae treated effluent. In general, the process of centrifugation will remove those solids which were heavier in the medium but left lighter solids in the centrifuged supernatant. Although centrifugation process is effective in removing most of the large/heavy solids from water, light and smaller size particles left in the centrifuged

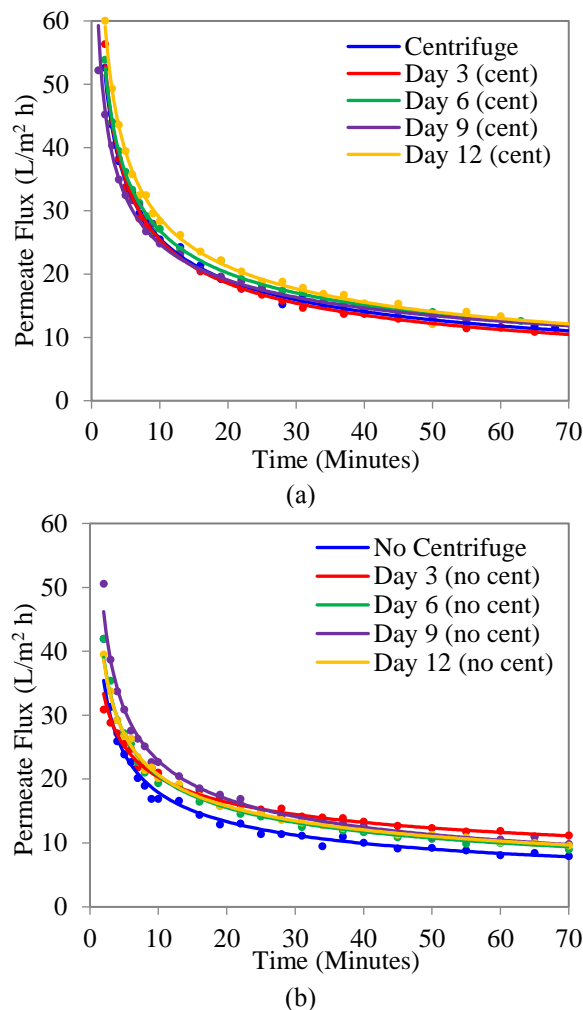


Fig. 3 Flux profile of ultrafiltration (a) with centrifugation and (b) without centrifugation

supernatant limits its application in AnPOME treatment.

Ineffectiveness of centrifugation findings have been observed and reported by Wong and team (2002). Wong and team (2002) pretreated the POME before the membrane operation with three different separate method namely filtration, centrifugation, and coagulation. It was found that centrifugation was able to produce the best pretreated sample quality in reducing total nitrogen, SS, turbidity, and colour as much as an average of 68.3% compared to filtration and coagulation which is 10.1% and 68%, respectively. However, the final quality of the centrifugation-UF system was not as remarkable due to the remaining small size particles left in the centrifuged supernatant whereby the potential for membrane fouling would be higher. The light solids in this study might probably had smaller molecules diameter than NF membrane's pore diameter, thus, the molecules can enter most pores, deposited over the pore walls. As a result, the volume of NF membrane pores decreased proportionally to the filtered volume, resulting in severe fouling.

Despite the flux profile of NF membrane at day 0 of microalgae treatment, Fig. 4a showed the similar trend as in Fig. 3a in which the water flux of NF membrane in filtering the centrifuged microalgae treated effluent was increased

with the increasing of microalgae treatment RT. The water flux was recorded as 11.64 L/m² h at day 3 of microalgae treatment RT and it was eventually increased to 12.12 L/m² h, 12.76 L/m² h, and 13.54 L/m² h at day 6, day 9, and day 12 of microalgae treatment RT, respectively. This observation was accounted by the same phenomenon. In general, almost all microorganisms including microalgae, bacteria, and fungi were able to produce a gel-like and highly hydrated matrix, EPS surrounding the cell (Singha 2012). These EPS on the microalgae outer cell will act as “glue” in keeping the microalgae together. With the growing of microalgae during treatment with RT, larger microalgae population inside the medium will therefore promoting the adhesion of particulates, thus eventually formed the large aggregates and removed during centrifugation. Therefore high SS removal through centrifugation would reduce the fouling propensity of NF membrane resulted in better water flux.

According to Alzahrani *et al.* (2013), when pH was adjusted from 3 (acidic) to 10 (alkaline) for NF and RO membrane studies, flux reduction or fouling would decline revealing that flux was improved at higher pH. This was because when pH became higher than 9, it could also lead to lower zeta potential of the membrane (influenced by pH), thus result in an increase of negatively charged membrane surface. This would repel against the cake layer formed on membrane surface allowing easier passage of water to pass through thus improving the flux of NF membrane. However in this study, as the pH of the medium increased with RT due to the uptake of carbon dioxide by microalgae, the water flux did not improved as predicted. By referring to Fig. 4b, the water flux in filtering microalgae treated effluent without centrifuged was recorded as 7.62 L/m² h which had slightly higher flux profile compared to NF membrane after centrifuged at day 0 of microalgae treatment initially. However, the advantage of non-centrifuged microalgae treated effluent did not last long as the highest water flux achieved was on day 6 of RT as recorded with 10.64 L/m² h. Prolonged microalgae treatment without centrifugation still resulted in the thickening of cake layer formation which eventually restricted the passage for water to pass through. Although with high pH condition which should help to reduce the fouling propensity of the membrane, cake layer formation was still predominant in affecting the flux profile. Therefore, the effect of pH was not obvious and the difference between membrane’s flux profiles at different RT was not for too different.

4.1.3 Reverse osmosis (RO)

From Fig. 5, a rather similar trend of flux profiles for RO membrane were observed when compared with UF membrane in Fig. 3. It cannot be denied that centrifugation played a certain role in reducing membrane fouling by pore blocking or cake layer formation that would lead to the increase of RO membrane permeation resistance. This was shown in Fig. 5a where the highest flux reached 11.52 L/m² h on day 12 of RT. In general, based on the flux profiles from Fig. 3a, 4a, and 5a, centrifugation was proficient in improving the flux performance on microalgae treated effluent for UF, NF, and RO membranes. Yu and team

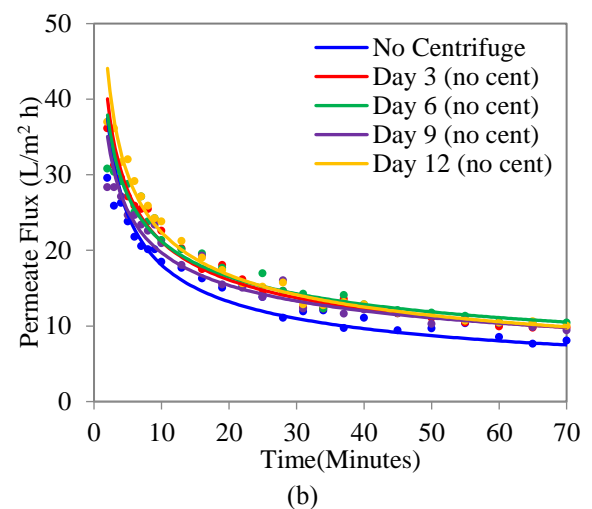
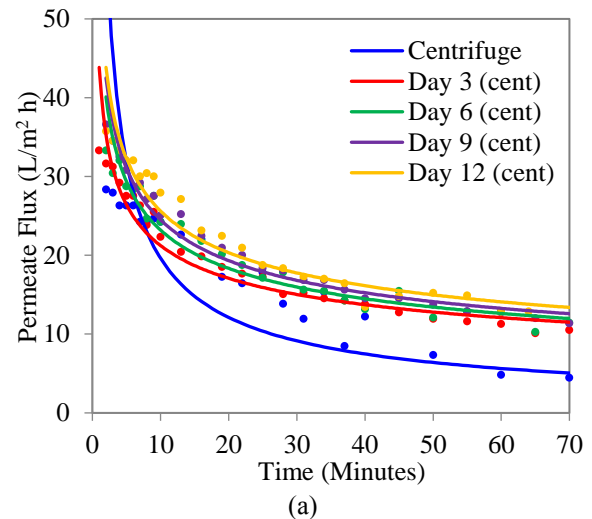


Fig. 4 Flux profile of nanofiltration (a) with centrifugation and (b) without centrifugation

(2009) identified that not just EPS that tightly bound to the cell walls of microalgae or bacteria (TB-EPSs) but those loosely bound EPSs (LB-EPSs) exudated by them also acted as natural flocculants to aggregate suspended particulates through sweep flocculation and bridging mechanism which further promoted heavier particulate sediments during centrifuged.

When comparison was made between centrifuged and non-centrifuged microalgae treated effluent on RO membrane, the difference in flux profiles was not as obvious as UF and NF membranes. Slightly higher flux of 8.31–11.52 L/m² h was observed by centrifuged microalgae treated effluent while lower flux of 6.64–9.28 L/m² h could be seen in non-centrifuged microalgae treated effluent at the end of filtration. Although cake layer did induced certain degree of hydraulic resistance onto RO membrane permeation, the removal of large particles after centrifugation still showed a slight difference in flux. The reason behind might be that cake layer formation was not the predominant fouling mechanism affecting the permeated flux. Instead, another fouling phenomenon attributed by concentration polarization was affecting the flux profile. Due to the tight surface structure posed by RO membrane,

the increase of osmotic pressure between boundaries adjacent to RO membrane surface formed from accumulated particulates like microalgae and EPSs that resulted in back transfer of water to the bulk solution reducing the permeated flux. Luo and Ding (2011) showed NF membrane (NF270), a polyamide membrane, produced lower permeated flux due to concentration polarization that was affected by high pH condition and transmembrane pressure (TMP) on dairy wastewater. In this study, RO membrane showed higher concentration polarization effect as higher TMP of 10 bars was used alongside with increasing pH.

While RO membrane filtering centrifuged microalgae treated effluent still showed increasing water flux with RT, RO membrane filtering non-centrifuged microalgae treated effluent showed otherwise. The highest water flux could be achieved by RO membrane without centrifuged was 9.51 L/m² h on day 6 of RT. Without centrifugation, cake layer formation together with concentration polarization finally cancelled out the positive effects of high pH which was suppose to mitigate fouling on RO membrane. Combination of biofouling and concentration polarization was recognized Chong and team (2008) as biofilm enhanced concentration polarization (BEOP) where concentration polarization was enhanced biofilm that increased the hydraulic resistance on RO membrane surface that eventually led to a slight decrease of flux after day 6 of RT as shown in Fig. 5b.

4.2 Hermia's model analysis

The flux profile resulting from successive filtration of each membrane (UF, NF, and RO) in filtering both centrifuged and non-centrifuged microalgae treated effluent presented in Fig. 3-5 showing a decline in membrane instantaneous flux over a period of time, which resulted from membrane fouling. The visible curve of permeate flux profile could be divided into two parts: Region I, the rapid initial drop followed by gradual decrease of flux with the increasing of operating time; and Region II, steady flux in which the flux profile shown a plateau straight line near the end of membrane filtration process (Abdelrasoul *et al.* 2013).

In order to identify the fouling mechanism of each filtration process under different experimental conditions, Hermia's model was applied to fit the experimental results. Table 2 summarized the two parameters determined using various Hermia's model that were the correlation coefficient (R^2) and value of constant k . The correlation coefficient (R^2) in Table 2 gave an indication on the predominant fouling mechanism (cake layer formation, intermediate blocking, standard blocking, and complete blocking) that influences the flux decline of each filtration process. Whereas for k constant value, it can be interpreted as a scaling factor that is proportional to concentration of pollutants as described by Blankert and team (2006) or the severity of membrane fouling as explained by Vincent Vela and team (2009). It was depicted that gradual reduction of the permeate flux over time in this work has a good correlation with cake layer formation ($n = 0$), demonstrated by the highest R^2 value among all fouling mechanisms regardless of the employment of centrifugation pretreatment

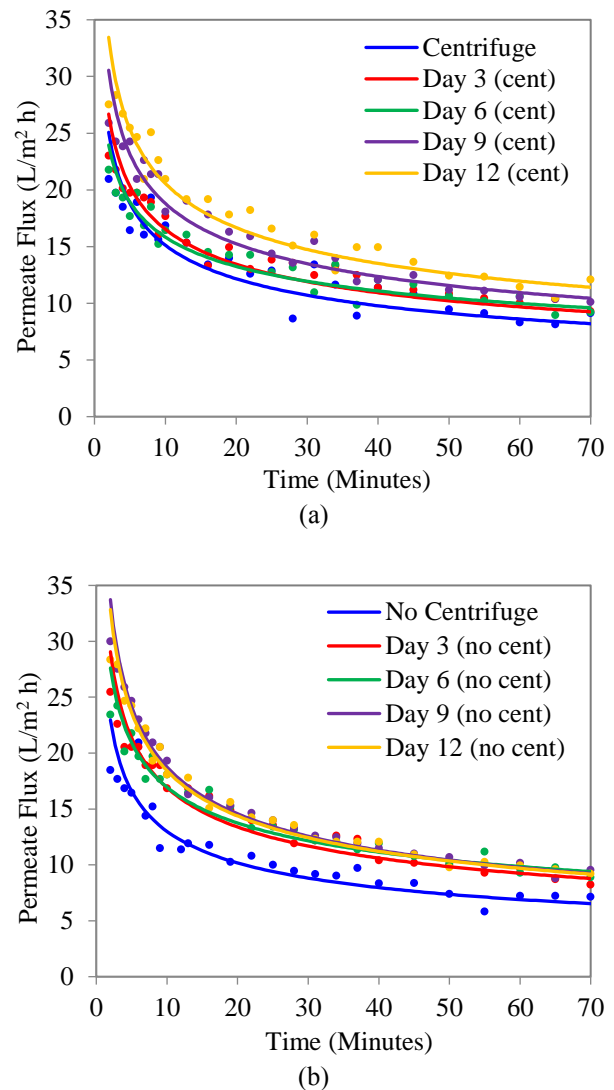


Fig. 5 Flux profile of reverse osmosis (a) with centrifugation and (b) without centrifugation

process and the RT of microalgae treatment, except the NF of centrifuged AnPOME at day 0 of RT.

Basically, palm oil mill wastewater contains high concentration of large solid aggregates compared to the membrane pores, in which external fouling on membrane would drastically happen. Integration of microalgae pretreatment prior membrane filtration has further put forward in promoting the number of solid aggregates in microalgae treated effluent due to biomass produced from bacteria or microalgae growth. Besides that, strong adhesion properties on EPS exudates by microalgae also encourage cake layer formation by coagulating particulates and microalgae cells towards wider diameter than membrane's pore size that easily accumulated on the surface of the membrane. The configuration of membrane filtration also played a role in accelerating the formation of cake layer. Since dead end filtration mode was used in this study, as the feed flow was forced perpendicularly through the membrane by hydrodynamic drag force exerted using high pressure. This would leave those retained particles

with no choice but to accumulate on the surface of the membrane. Eventually, cake thickness build-up with time thus resulted in the decrease of permeate flux.

As aforementioned that all permeate flux decline showed good correlation with cake layer formation except NF membrane filtering centrifuged AnPOME at day 0 of RT which showed a different fouling mechanism that was standard pore blocking ($n=1.5$) or otherwise known as internal adsorption fouling. One probability as standard pore blocking only observed on NF membrane filtering centrifuged AnPOME at day 0 of RT was the removal of heavier solids through centrifugation that remain some micropollutants like dissolved organic carbon (DOC) or tannin from AnPOME that manage to adsorb onto NF membrane pores wall. However, such incident did not occurred on UF membrane which was supposed to as it have larger pore size that NF membrane. Some studies found that UF membrane main fouling mechanism was adsorption initially followed by cake layer whereas NF membrane fouling was mainly contributed by external fouling like cake layer while filtering micropollutants (Acero *et al.* 2010). In contrast, another study done by Rickman and team using 50 kDa polyethersulfone (PES) UF membrane, 0.22 μm mixed-cellulose ester (MCE) microfiltration (MF) membrane and 5 μm MCE MF membrane showed that 5 μm MF membrane (largest pore size membrane) did not had irreversible resistance but was formed with cake layer of whole algal cells on the membrane surface that still allowed microparticles and macroparticles to pass through. As for 50 kDa UF membrane and 0.22 μm MF membrane, irreversible fouling was observed instead (Rickman *et al.* 2012). Perhaps those micropollutants did not adsorb onto UF membrane pore walls suggesting that the pore size of 10 kDa might be large enough to pass through which remained a higher flux of 12.35 $\text{L}/\text{m}^2 \text{ h}$ (Fig. 3a). On the other hand, 5.20 $\text{L}/\text{m}^2 \text{ h}$ flux (Fig. 4a) which was shown by NF membrane on day 0 of RT with centrifuged AnPOME in this study, suggested severe internal fouling was happening thus resulted in very low flux. As for RO membrane when filtering centrifuged AnPOME at day 0 of RT, due to the tight structure with small pore size, less adsorption resistance was observed.

Besides values of R^2 , Table 2 also showed the k constant value of each fitted parameters of Hermia's models from experimental results for UF, NF, and RO membrane. According to the definition explained from Section 2 in Hermia's model, k value seems to represent the fouling severity on the membrane by foulants. In this study, it was consistent with constant k value from cake layer formation, K_g , intermediate blocking model, K_i , and standard blocking model, K_s except complete blocking model, K_c that showed slight value reduction with RT. As RT increased, nutrient reduction uptake by microalgae could be observed in centrifuged and non-centrifuged microalgae treated effluent that might reduce the fouling propensity. As for non-centrifuged microalgae treated effluent, although the concentration of SS increased in with RT, due to the increased size of foulant aggregates promoted by microalgae's EPSs, it also helped mitigate some fouling tendency. Nonetheless, those k values did not followed a

clear trend with RT as it might be dependent on different condition like TMP, temperature or density of feed solution during filtration (Vincent Vela *et al.* 2009).

4.3 Resistance-in-series model analysis

While Hermia's models were used in identifying the predominant mechanism during fouling, resistance-in-series model, which was more experimentally dependence, was used to determine the dominant resistance components that caused the flux decline in this study. The four resistance components in resistance-in-series are concentration polarization resistance, adsorption resistance, cake layer resistance and membrane hydraulic resistance.

Based on Fig. 6, it can be deduced that the main fouling factor for UF and NF membrane filtration processes were governed by R_g and R_c . At the beginning of filtration, the fouling of a UF/NF membrane was clearly revealed by the considerable permeate flux decline, which attributed to the rapid deposition of fine particles from suspension on the membrane surface and subsequently penetrate into the membrane pores and thus accumulate. This type of fouling mechanism is likely to be physically irreversible, which cannot be totally eliminated by physical cleaning or certain pretreatment. As the time of operation progresses and under high operating pressure (5 bars for UF and 7 bars for NF), the gradual accumulation of solutes over the membrane surface leading to severe concentration polarization. The slower flux decline at later stages was then leads to the eventual formation of cake layer on the membrane surface. In view of the similar percentage of R_g and R_c in a UF/NF membrane filtration process implies that more than one type of blocking mechanism is involved in a single process. This postulation was in good agreement with the finding of Sarkar (2013) who claimed that the fouling by particulates appears to be caused by several simultaneous mechanisms. Moreover, as this work was carried out using a laboratory bench-scale dead end test unit, R_c resulted from the accumulation of solutes over the membrane surface was occurred more apparently when the volume of retentate decrease progressively with time due to the increasing of feed concentration. In view of this, the percentage of R_c was as compatible as the percentage of R_g in a UF/NF membrane filtration process.

Whereas, for RO membrane, R_c solely was the predominant membrane fouling factor regardless microalgae treatment RT and centrifugation. This might be due to the tighter RO membrane structure coupled with high TMP 10 bars applied for RO membrane filtration process. High TMP during RO membrane filtration process would accelerate the concentration polarization effect on RO membrane surface where the particulates being forced near to the membrane surface and creating high concentration gradient than the bulk solution. Concentration polarization could also be greatly enhanced with the formation of cake layer on RO membrane surface in which this phenomenon was called cake-enhanced osmotic pressure (CEOP) phenomenon. Due to CEOP phenomenon, the solid particles slowly diffuse through the evermore difficult and twisted path within the cake layer adding more hydraulic resistance

Table 2 Values of k and correlation coefficient (R^2) based on various blocking mechanism model equations for flux reduction at 5 bars, 7 bars, and 10 bars for ultrafiltration, nanofiltration, and reverse osmosis membrane, respectively

Retention Time (day)	Centrifugation	Type of Membrane	$n = 0$		$n = 1.0$		$n = 1.5$		$n = 2.0$	
			k_4	R^2	k_3	R^2	k_2	R^2	k_1	R^2
Day 0	Yes	UF	0.0001	0.9867	0.0010	0.9502	0.0022	0.9175	0.0196	0.8785
		NF	0.0011	0.9107	0.0026	0.9737	0.0030	0.9871	0.0171	0.9673
		RO	0.0002	0.9726	0.0009	0.9608	0.0015	0.9485	0.0096	0.9300
	No	UF	0.0002	0.9734	0.0010	0.9073	0.0017	0.8581	0.0117	0.8035
		NF	0.0003	0.9935	0.0014	0.9872	0.0021	0.9679	0.0135	0.9385
		RO	0.0003	0.9680	0.0010	0.9395	0.0013	0.9121	0.0075	0.8834
Day 3	Yes	UF	0.0001	0.9835	0.0011	0.9470	0.0023	0.9087	0.0203	0.8665
		NF	0.0001	0.9965	0.0009	0.9874	0.0019	0.9759	0.0158	0.9587
		RO	0.0002	0.9851	0.0009	0.9719	0.0014	0.9573	0.0099	0.9421
	No	UF	0.0001	0.9858	0.0008	0.9601	0.0015	0.9374	0.0119	0.9135
		NF	0.0001	0.9889	0.0010	0.9711	0.0019	0.9465	0.0146	0.9140
		RO	0.0002	0.9937	0.0009	0.9773	0.0015	0.9594	0.0105	0.9372
Day 6	Yes	UF	0.0001	0.9886	0.0010	0.9525	0.0022	0.9215	0.0211	0.8906
		NF	0.0001	0.9899	0.0009	0.9832	0.0018	0.9707	0.0154	0.9542
		RO	0.0001	0.9711	0.0007	0.9554	0.0012	0.9405	0.0083	0.9228
	No	UF	0.0001	0.9652	0.0009	0.9211	0.0017	0.8809	0.0135	0.8385
		NF	0.0001	0.9883	0.0009	0.9734	0.0018	0.9568	0.0143	0.9339
		RO	0.0001	0.9793	0.0008	0.9643	0.0014	0.9472	0.0097	0.9253
Day 9	Yes	UF	0.0001	0.9910	0.0010	0.9593	0.0023	0.9325	0.0213	0.9006
		NF	0.0001	0.9985	0.0009	0.9893	0.0019	0.9769	0.0165	0.9599
		RO	0.0001	0.9874	0.0008	0.9743	0.0015	0.9600	0.0110	0.9404
	No	UF	0.0001	0.9744	0.0010	0.9329	0.0020	0.8927	0.0165	0.8475
		NF	0.0001	0.9847	0.0009	0.9700	0.0017	0.9519	0.0128	0.9275
		RO	0.0002	0.9950	0.0009	0.9623	0.0016	0.9372	0.0119	0.9085
Day 12	Yes	UF	0.0001	0.9913	0.0010	0.9545	0.0024	0.9242	0.0229	0.8878
		NF	0.0001	0.9911	0.0008	0.9874	0.0019	0.9800	0.0173	0.9668
		RO	0.0001	0.9829	0.0008	0.9715	0.0016	0.9606	0.0125	0.9453
	No	UF	0.0001	0.9748	0.0009	0.9373	0.0018	0.9054	0.0139	0.8660
		NF	0.0001	0.9889	0.0010	0.9696	0.0020	0.9457	0.0163	0.9150
		RO	0.0002	0.9935	0.0009	0.9628	0.0016	0.9399	0.0118	0.9132

causing higher concentration gradient difference that back transport from the fouled RO membrane to the bulk solution (Tang *et al.* 2011).

The occurrence of internal adsorption fouling phenomenon that occurred on NF membrane filtering centrifuged AnPOME at day 0 concluded from Hermia's model was in agreement with the analysis of resistance-in-series model where the highest R_a was found to be 29.16% in Fig. 6. As interpreted in Hermia's model, it was due to centrifugation process that retained trace amount of micropollutants that caused internal pore clogging while UF membrane had a larger pore size that permit most micropollutants to pass by before cake layer settle in and with the tight structure of RO membrane that made adsorption nearly impossible. However, from resistance-in-series model analysis, RO membrane illustrated a rather high R_a with 6.26% to 15.88% although R_c and R_g was still

the predominant fouling component when compared to UF and NF membrane. The likelihood depicted by Bacchin and Aimar's (2005) work was an irreversible transition condition that occurred as a result of concentration polarization that form a new solid phase of monolayer or multilayer fouling on the RO membrane surface. As high TMP of 10 bars and CEOP fall on the solid particles accumulated on RO membrane surface, spinodal decomposition appeared when Van der Waals attraction counterbalance repulsion leading to an instability forming aggregates that was irreversible by physical cleaning. This thus resulted in a slight increase of adsorption resistance.

5. Conclusions

Effect of RT on permeate flux profiles of two stages microalgae/membrane system did showed increment in flux

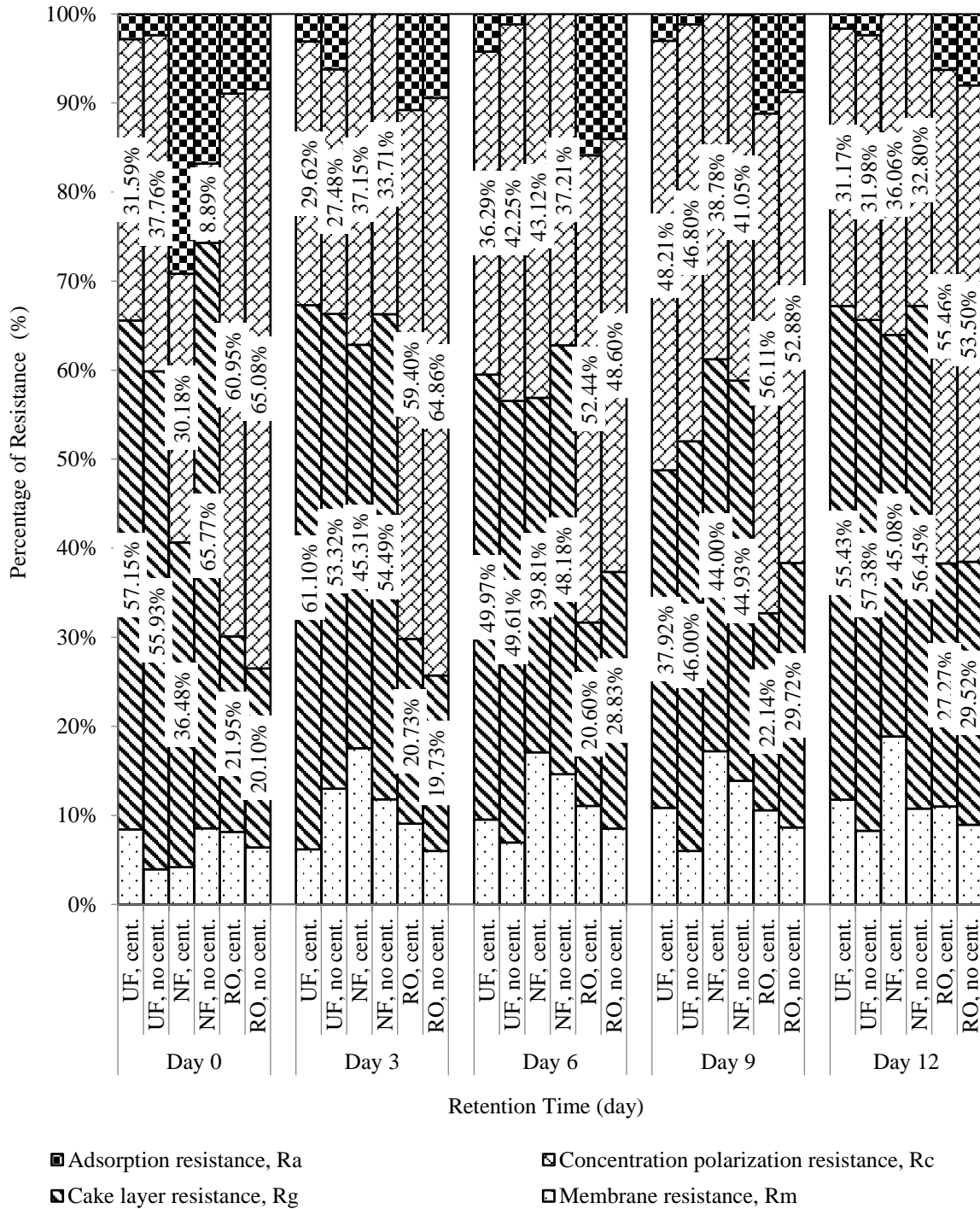


Fig. 6 Fouling resistance of ultrafiltration, nanofiltration, and reverse osmosis membrane based on resistance-in-series model

performance as the treatment period got longer. In which UF membrane showed the best flux performance with highest flux of 12.35 L/m² h on 5 bars TMP while the highest flux for NF and RO membrane was with 13.54 L/m² h on 7 bars TMP and 11.52 L/m² h on 10 bars TMP respectively on centrifuged microalgae treated effluent at RT of day 12. With the help of centrifugation in reduction of SS from microalgae treated effluent before passing through membrane, it had a much predicted trend with RT. This work revealed that without centrifugation, flux

performance would decline at longer RT mostly after day 9 of RT due to the increased microalgae biomass that formed cake layer on the surface of all membrane. Biofouling behavior was identified through Hermia's model in which fouling of UF and NF membrane was mainly caused by cake layer formation and it was also supported by the analysis for resistance-in-series model. However in RO membrane it was concentration polarization as the dominating fouling factor. By identifying the fouling manners occurred in UF, NF, and RO membrane in this

study, further fouling mitigation and cleaning strategies could be applied for the improvement of flux and performance of the new innovative two stages microalgae/membrane filtration system.

Acknowledgments

The authors wish to gratefully acknowledge the financial support for this work by Geran Universiti Penyelidikan (GUP-2017-098) and Dana Penyelidikan Strategik (KRA-2017-016). The authors also wish to acknowledge the Ministry of Education Malaysia for sponsoring Z.H. Wong postgraduate studies via MyBrain.

References

- Abdelrasoul, A., Doan, H. and Lohi, A. (2013), "Fouling in membrane filtration and remediation methods", *Mass Transfer - Advances in Sustainable Energy and Environment Oriented Numerical Modeling, InTech, Rijeka, Croatia*.
- Acero, J.L., Benitez, F.J., Teva, F. and Leal, A.I. (2010), "Retention of emerging micropollutants from UP water and a municipal secondary effluent by ultrafiltration and nanofiltration", *Chem. Eng. J.*, **163**(3), 264-272.
- Alzahrani, S., Mohammad, A.W., Hilal, N., Abdullah, P. and Jaafar, O. (2013), "Identification of foulants, fouling mechanisms and cleaning efficiency for NF and RO treatment of produced water", *Sep. Purif. Technol.*, **118**, 324-341.
- Bacchin, P. and Aimar, P. (2005), "Critical fouling conditions induced by colloidal surface interaction: From causes to consequences", *Desalination*, **175**(1), 21-27.
- Blankert, B., Betlem, B.H.L. and Roffel, B. (2006), "Dynamic optimization of a dead-end filtration trajectory: Blocking filtration laws", *J. Membr. Sci.*, **285**(1-2), 90-95.
- Bowen, W.R., Calvo, J.I. and Hernández, A. (1995), "Steps of membrane blocking in flux decline during protein microfiltration", *J. Membr. Sci.*, **101**(1-2), 153-165.
- Chong, T., Wong, F. and Fane, A. (2008), "The effect of imposed flux on biofouling in reverse osmosis: Role of concentration polarisation and biofilm enhanced osmotic pressure phenomena", *J. Membr. Sci.*, **325**(2), 840-850.
- Czarczyk, K. and Myszka, K. (2007), "Biosynthesis of extracellular polymeric substances (EPS) and its role in microbial biofilm formation", *Pol. J. Environ. Stud.*, **16**(6), 799-806.
- de Barros, S.T.D., Andrade, C.M.G., Mendes, E.S. and Peres, L. (2003), "Study of fouling mechanism in pineapple juice clarification by ultrafiltration", *J. Membr. Sci.*, **215**(1-2), 213-224.
- Hermia, J. (1982), "Constant pressure blocking filtration laws—Application to power-law non-newtonian fluids", *Trans. Inst. Chem. Eng.*, **60**(3), 183-187.
- Hoskins, D.L., Stancyk, S.E. and Decho, A.W. (2003), "Utilization of algal and bacteria extracellular polymeric secretions (EPS) by the deposit-feeding brittlestar *Amphipholis gracillima* (Echinodermata)", *Mar. Ecol. Prog. Ser.*, **247**, 93-101.
- Kołtuniewicz, A.B. and Field, R.W. (1996), "Process factors during removal of oil-in-water emulsions with cross-flow microfiltration", *Desalination*, **105**(1-2), 79-89.
- Li, Y., Zhou, W., Hu, B., Min, M., Chen, P. and Ruan, R.R. (2011), "Integration of algae cultivation as biodiesel production feedstock with municipal wastewater treatment: Strains screening and significance evaluation of environmental factors", *Bioresour. Technol.*, **102**(23), 10861-10867.
- Lim, A.L. and Bai, R. (2003), "Membrane fouling and cleaning in microfiltration of activated sludge wastewater", *J. Membr. Sci.*, **216**(1-2), 279-290.
- Luo, J. and Ding, L. (2011), "Influence of pH on treatment of dairy wastewater by nanofiltration using shear-enhanced filtration system", *Desalination*, **278**(1-3), 150-156.
- Mohammadi, T., Kazemimoghadam, M. and Saadabadi, M. (2003), "Modeling of membrane fouling and flux decline in reverse osmosis during separation of oil in water emulsions", *Desalination*, **157**(1-3), 369-375.
- Rickman, M., Pellegrino, J. and Davis, R. (2012), "Fouling phenomena during membrane filtration of microalgae", *J. Membr. Sci.*, **423-424**, 33-42.
- Sarkar, B. (2013), "A combined complete pore blocking and cake filtration model during ultrafiltration of polysaccharide in a batch cell", *J. Food Eng.*, **116**(2), 333-343.
- Singha, T.K. (2012), "Microbial extracellular polymeric substances: Production, isolation and application", *IOSR J.Pharm.*, **2**(2), 276-281.
- Tang, C.Y., Chong, T.H. and Fane, A.G. (2011), "Colloidal interactions and fouling of NF and RO membranes: A review", *Adv. Colloid Interface Sci.*, **164**(1-2), 126-143.
- Turano, E., Curcio, S., Paola, M.G.D., Calabrò, V. and Iorio, G. (2002), "An integrated centrifugation-ultrafiltration system in the treatment of olive mill wastewater", *J. Membr. Sci.*, **209**(2), 519-531.
- Yu, G.H., He, P.J. and Shao, L.M. (2009), "Characteristics of extracellular polymeric substances (EPS) fractions from excess sludges and their effects on bioflocculability", *Bioresour. Technol.*, **100**(13), 3193-3198.
- Vela, M.C.V., Blanco, S.Á., García, J.L. and Rodríguez, E.B. (2009), "Analysis of membrane pore blocking models adapted to crossflow ultrafiltration in the ultrafiltration of PEG", *Chem. Eng. J.*, **149**(1-3), 232-241.
- Wong, P.W., Sulaiman, N.M., Nachiappan, M. and Varadaraj, B. (2002), "Pre-treatment and membrane ultrafiltration using treated palm oil mill effluent (POME)", *J. Sci. Technol.*, **24**, 891-898.

CC